



ARTICLE

Compressive Biomechanics of the Reptilian Intervertebral Joint

Kadi Fauble¹ James Adams¹ Maura Gerdes² Caroline VanSickle¹ Bruce A. Young^{1*}

1. Department of Anatomy, Kirksville College of Osteopathic Medicine, A.T. Still University, Kirksville, MO, USA.

2. Department of Internal Medicine, Kirksville College of Osteopathic Medicine, A.T. Still University, Kirksville, MO, USA.

ARTICLE INFO

Article history

Received: 5 August 2020

Accepted: 11 August 2020

Published Online: 31 August 2020

Keywords:

Stress

Displacement

Intervertebral joint

Varanus

Alligator

Articular facet

Bipedalism

ABSTRACT

This study compared the pre-sacral intervertebral joints of the American alligator (*Alligator mississippiensis*) with those from specimens of *Varanus*. These two taxa were chosen because they have similar number of pre-sacral vertebrae and similar body weights; however, *Varanus* can move bipedally and has diarthrotic intervertebral joints, whereas *Alligator* has intervertebral discs and cannot move bipedally. This study consisted of three objectives: (1) to document the anatomy of the intervertebral joint, (2) to quantify the compressive biomechanics of the intervertebral joints and explore which features contributed to compression resistance, and (3) to quantify the impact of compression on the intervertebral foramen and spinal nerves in these two taxa. The experimental results revealed that the diarthrotic intervertebral joints of *Varanus* were significantly (4x) stiffer than the intervertebral disc of *Alligator*, and that a significant component of this increased stiffness arose from the facet joints. Compressing the intervertebral joints of the two taxa caused a reduction in foraminal area, but the magnitude of this reduction was not significantly different. We hypothesize that the main factor preventing spinal nerve impingement in *Varanus* during gravitational compression is the relatively small size of the spinal ganglion/nerve relative to the foraminal area.

1. Introduction

During their long evolutionary history many clades of reptiles have transitioned between different locomotor modes. Crocodylians have repeatedly re-invaded the aquatic realm, and terrestrial forms have transitioned from quadrupedal to bipedal locomotion^[1]. The varanoid lizards have a complex pattern of multiple re-invasions of aquatic and terrestrial habitats^[2]. One consequence of these transitions is easily seen in limbs, with the repeated transition between a cursorial manus or pes, and

an aquatic flipper^[3,4]. The consequences in the vertebral column have not been studied as heavily, but in crocodylians there is a clear “stiffening” of the vertebral column associated with terrestrial locomotion^[5,6]. The bony osteoderms of crocodylians combine with the intervertebral joint to influence both dorso-ventral and lateral flexion of the trunk^[7].

One attribute of the crocodylian vertebral column thought to influence stiffness is the presence of an intervertebral disc^[7]. In archosaurs, which include crocodylians, the intervertebral disc includes fibrocartilage

*Corresponding Author:

Bruce A. Young,

Department of Anatomy, Kirksville College of Osteopathic Medicine, A.T. Still University, Kirksville, MO, USA;

Email: byoung@atsu.edu

surrounding a nucleus pulposus core^[8]. The nature of the intervertebral joint in other reptiles is less understood, particularly among squamate reptiles where the intervertebral disc is absent and the joint is described as diarthrotic or amphiarthrotic^[9,10]. Previous studies have emphasized the role of the reptilian intervertebral joint in vertebral flexibility^[11,12], but little is known about how these joints respond to compression. Gravitational compression is an unavoidable consequence of bipedalism. Bipedalism evolved repeatedly in dinosaurs^[13], and in extinct crocodylians^[14], but is not characteristic of living crocodylians. Several squamate groups have evolved bipedal posturing and locomotion^[15], interestingly, among varanid lizards (the largest of all squamates) bipedalism only occurs in the forms with the largest body sizes^[16].

The purpose of this study was to compare the response of a squamate (*Varanus*) and non-squamate (*Alligator*) intervertebral joint to gravitational compressive loads. This was done by comparing the compressive stress/strain curves^[17,18,19] and using a variety of anatomical and imaging techniques to quantify the displacements at the intervertebral joint^[20,21]. This study considers two intervertebral joints: the centrum joint (where the intervertebral disc is in *Alligator*) and the facet joint between the prezygapophysis and the postzygapophysis. In most reptiles the facet joint is in the frontal plane^[8] and is thought to play a role in limiting dorso-ventral flexion and vertebral torsion^[22]. Previous studies in humans and other mammals have shown that compressive forces can reduce the dimensions of the intervertebral foramen leading to impingement of the spinal nerve^[23,24]. This study quantifies the intervertebral foramen of *Varanus* and *Alligator*, and how that portal changes when exposed to compressive loads. More specifically, this work tests three hypotheses: 1) The morphological differences in the centrum intervertebral joint between *Varanus* and *Alligator* results in significant differences in compliance across this joint; 2) Translational displacement in the frontal plane at the facet intervertebral joint plays an important role in compliance across the joint in *Varanus* and *Alligator*; and 3) The intervertebral disc of *Alligator* reduces gravitation-induced distortion of the intervertebral foramen compared to that of *Varanus*.

It is important to note the restricted scope of this study. Previous studies have examined the biomechanics of the vertebral cancellous and compact bone^[25-27]. Similar studies have quantified the biomechanical properties of hyaline cartilage^[28] and fibrocartilage^[29]. Rather than focus on these structural features, this study examines the compressive forces acting over the

space or gap between adjacent vertebrae. This focus has been previously included in the (more limited) studies of synovial biomechanics^[30]. By studying how the intervertebral joint compresses and the associated facet joints shift, we are effectively studying what is treated as the “pre-load” phase for some studies of vertebral biomechanics. One important consequence of this study being restricted to the displacement of the intervertebral joints is that the strains we detail are much higher, and the stresses much lower, than in studies of compression of the vertebrae.

2. Materials and Methods

2.1 Live Animals

Five live sub-adult (165 - 183 cm total length) American alligators (*Alligator mississippiensis*) were obtained from the Louisiana Department of Wildlife and Fisheries. The animals were housed communally in a 29 m² facility that featured three submerging ponds, natural light, and artificial lights on a 12:12 cycle. The facility was maintained at 30 - 33° C. Warm water rain showers were provided every 20 minutes, which helped maintain the facility at > 75% relative humidity. The alligators were maintained on a diet of previously frozen adult rats. The husbandry and use of the live alligators followed all applicable national guidelines, and was approved by the IACUC of A.T. Still University (Protocols #208 and #209).

Five monitor lizards were obtained from commercial vendors: two *Varanus salvator* (total lengths of 113 and 146 cm), two *Varanus niloticus* (total lengths of 126 and 136 cm), and one specimen of *Varanus panoptes* (total length = 138 cm). These three species are all known to stand/locomote in a vertical (bipedal) fashion^[16]. The lizards were housed in individual terraria within a special reptile holding facility with a 12:12 light cycle, water *ad libitum*, and a temperature range of 28 to 32° C. The animals were maintained on a diet of previously frozen rodents. The housing, care, and use of the live *Varanus* followed all applicable national guidelines and were approved by the Institutional Animal Care and Use Committee of A.T. Still University (Protocol #175).

2.2 Specimen Collection

Individuals were euthanized using a combination of Isoflurane anesthesia and cardiac excision. Immediately after euthanasia the three most caudal trunk vertebrae (i.e., the three vertebrae immediately cranial to the sacral vertebra) were excised preserving two successive intervertebral joints and the majority of the three vertebrae. The excised biomechanics block was skinned, but no additional dis-

section was performed. Three other sample blocks were removed. Each block consisted of three vertebrae and two intervertebral joints, and the sample blocks were removed in the same sequence from each animal with no skipped vertebrae. The block immediately cranial to the biomechanics block was designated the MRI block, followed (cranially) by the CT block, and finally the Histology block.

2.3 Morphological Analyses

The MRI block was placed in a custom-built vise capable of compressing the block but containing no metal components. The MRI block and vise were placed in a phased-array surface coil then imaged with a clinical 0.35-T MRI unit (Ovation, GE Medical Systems, Milwaukee, Wisconsin, USA) (Sagittal T1-weighted 3D fast spoiled gradient, 38.9/14.6, flip angle 30 degrees, field of view 80 mm, slice 2 mm, matrix 320x224, Nex 3, scan time 10 min 47 sec).

Each MRI block was subjected to three MRI scans, each at a different level of compression; minimal compression (just enough to hold the block in the vise), moderate compression, and maximum compression. The latter two levels were based on the feeling of resistance of the MRI block in the vise during compression by hand, and visual evaluation of shortening of the block. Each MRI image was imported into ImageJ (NIH) where the area of the intervertebral foramen was quantified. Using a mid-sagittal slice we also defined a vertebral unit length which was the cranial-caudal length of one vertebra and intervertebral joint.

The histology blocks were immediately placed in 10% neutral-buffered formalin (NBF), the CT blocks were compressed in a C-clamp then placed in NBF. Post-fixation the histology and CT blocks were imaged using a clinical 64-detector CT unit (Ingenuity, Philips Medical, Andover, Massachusetts, USA) captured through helical acquisition at 0.67 mm, FOV 160 mm, 100 kV, 125 mAs, with a rotation time of 500 msec, section thickness of 0.67 mm, and pitch of 0.391. The DICOM images were imported into Osirix (Pixmeo SARL, Geneva, Switzerland) for 3D reconstruction, then individual images exported to ImageJ. Using ImageJ the surface area of the intervertebral foramen and the distance between adjacent vertebrae were quantified.

The fixed histology and CT blocks were decalcified in RDO Rapid Decalcifier (Apex Engineering Products, Aurora, Illinois, USA) for 24 hours prior to dehydration and paraffin embedding. Parasagittal sections were cut (at 10 μ m) through the region of the intervertebral foramen and the articular processes. Mounted sections were stained

with either Hematoxylin and Eosin, or Masson's trichrome stain (following^[33]). Microscopic anatomy was documented using a DM 4000B microscope (Leica Microsystems Inc., Buffalo Grove, Illinois, USA). Images were imported into ImageJ and the area of the intervertebral foramen and the spinal nerve quantified.

Portions of the excised blocks not used for histological analysis were dissected, with an emphasis on the intervertebral foramen.

2.4 Compression Testing

The biomechanics block was placed, ventral surface down, on a glass plate coated with reptilian Ringers solution^[31] to minimize friction. The vertebral body on the cranial end of the block was abutted to a modified push rod on an infusion pump (901 Harvard Apparatus, Holliston, Massachusetts, USA). High-speed digital videography was used to ensure that the infusion pump could maintain a constant rate (0.02 mm/s) even against light resistance; this same system had been previously used for a study of the compressive biomechanics of snake skin^[32]. The vertebral body on the caudal end of the block was abutted to a force transducer (FT03 GRASS, West Warwick, Rhode Island, USA); the maximum range of which (20 kg) was never encountered in this study. The force transducer was coupled to a preamplifier (P122 GRASS), the output of which was recorded (at 1kHz sampling rate) using the MiDas data acquisition system (Xcitex Inc., Woburn, Massachusetts, USA).

Analyzing the compression data was complicated by the compound nature of the block, i.e. the blocks had both vertebral bodies of compact bone and intervertebral joints, the fact that the two intervertebral joints (at the centrum and facets) could both exhibit displacement, and by the complex 3-D shape of the centrum joint which precluded measuring the displacement in the intact material. When a compressive load is applied to one of the vertebral blocks, there is distinct shortening of that block, sometimes in excess of 10% of the resting length (Figure 1). Examination of the compressed block demonstrates that the cranial-caudal lengths of the vertebrae have not changed; in other words, the shortening is not due to compression of the vertebrae. The gap between successive spinous processes is visibly reduced (Figure 1) and there is visible displacement at the intervertebral facet joint (Figure 1). Our procedure was designed to measure the displacement at the intervertebral facet joint, which we will express as displacement in units of % facet length (the length being directly measured from CT images. This displacement would be resisted by two components: a minor component formed by the small

connective tissue surrounding the intervertebral facet joint, and the major component which is the intervertebral centrum joint. The centrum joint is (roughly) perpendicular to the plane of facet displacement, and so will undergo compression as the facet joint displaces. Our procedure will measure the resistance of both components; following convention we will express this resistance as stress (in units of kPa) by dividing the force measured by the force transducers by the surface area of the centrum intervertebral joint.

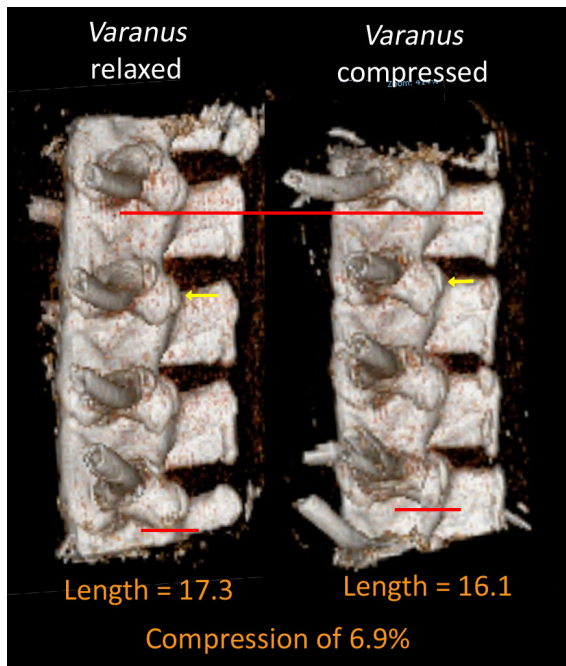


Figure 1. 3-D reconstruction of CT images of pre-sacral vertebrae of *Varanus salvator* at rest (left) and following compression with a C-clamp (right). Compression caused a shortening of 7%. This change in length was localized to the intervertebral joints, not the vertebral bodies. The major contributor to this compressive length reduction was displacement at the intervertebral facet joints (yellow arrows)

Operationally, this means that on the data traces that were recorded (Figure 2), we identified the point where the initial deflection in force gave rise to a linear relationship between force and displacement (linearity being determined using standard curve fitting protocols and R^2 maximization). This point is indicated by the lower red arrow in Figure 2, and was used as the 0,0 reference point. The same curve fitting protocols were applied to identify where the relationship between force and displacement deviated from linear (the upper arrow in Figure 2). From each data trace the maximum stress (the Y intercept of the upper arrow in Figure 2, after division by centrum cross-sectional area), maximum facet displacement (the X intercept of the upper arrow in Figure 2, after division by facet length), and stress

per unit displacement (the slope of the line between the two arrows in Figure 2) were quantified.

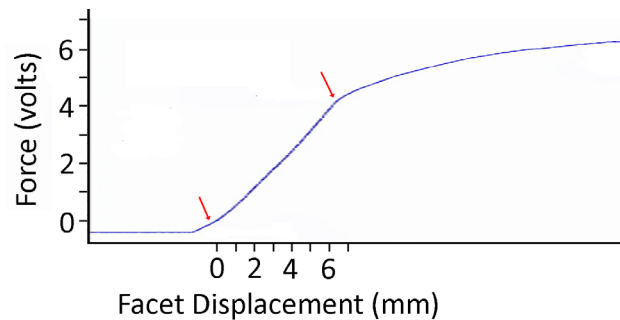


Figure 2. Raw data trace from a compression trial on *Alligator mississippiensis*. The upper and lower boundaries of the linear relationship between force and facet displacement are indicated with red arrows. Compression was terminated shortly after the upper deflection point was reached to avoid doing permanent damage to the specimen (or experimental apparatus)

Three trials were performed on each biomechanics block. Following these trials, the articular processes of the block were disrupted using a rongeur. This disruption greatly reduced/eliminated resistance at the intervertebral facet joint, while leaving the intervertebral centrum joint intact. Three additional compression trials were performed on each biomechanics block after the disruption of the articular processes. Each biomechanics block was photographed against a ruler and the photo imported into ImageJ (NIH) which was used to measure the cross-sectional area of the centrum; facet length for each block was measured from CT images.

2.5 Replica Vertebrae

The two most caudal pre-sacral vertebrae were removed from a previously prepared skeleton of an adult *Varanus salvator* from the private collection of BAY. Each vertebra was scanned (macro, full HD, 2- 360° scans and one filler scan) separately on a 3D laser scanner (2020i, NextEngine, Santa Monica, California, USA), scaled up to 3x the original size then 3D replicas printed (H800+, Afinia, Chanhassen, Minnesota, USA) using polyacetic acid filament PLA (Afinia). Epoxy couples were made to connect the replica vertebrae to the compression testing unit (detailed above); the epoxy was used to minimize the chance of damage to the replica vertebrae during repeated compression trials.

The first trials examined force transmission between adjacent vertebral bodies (that is, through the intervertebral joint). Consecutive trials were performed using first the bare replica vertebrae, and then inserting between the adjacent vertebral bodies: (1) a thin (1.0 mm) pad of sili-

cone, (2) a thick (3.0 mm) pad of silicone, and (3) a small sealed latex pouch of saline, designed to replicate a bursa or synovial joint capsule.

After the first series of trials, cyanoacrylate adhesive and a dense rubber pad were used to fix the articular processes in a non-compressed position (overlap between the articular facets limited to the cranial portion of the superior articular process). A second round of trials, in the same sequence as the first, were then performed. A third round of trials were intended to replicate the disrupted vertebrae (detailed above). Rather than crush the articular processes with a rongeur, the articular processes were cut off with a fine coping saw; the proximal ends of the cut articular processes could not make contact even at maximal compression. The third round of trials employed the same four states in the same sequence as the previous two trials. It should be noted that these replica vertebrae were treated in the same way as the experimental blocks; they had high strains and low stress values. At the end of the trials the artificial vertebrae were visually inspected and found to be unharmed, despite having undergone multiple rounds of compression.

3. Results

3.1 Anatomy

The pre-sacral vertebrae of *Alligator* had a mean length of 26.8 mm (s.d. = 1.1), while those of *Varanus* had a mean length of 18.5 mm (s.d. = 2.6); the greater size range of the specimens of *Varanus* produced more variation in vertebral length. The vertebrae of *Varanus* were significantly ($t = 6.70$, $n = 5$, $\rho = 0.00008$) shorter (cranial-caudal) than the vertebrae of *Alligator*. The reptilian intervertebral joint has two parts; the opposing surfaces of the centra, and the facet joint of the articular processes. The facets of *Alligator* are oriented 59° off of the horizontal, while the facets of *Varanus* are 49° off of the horizontal (Figure 3). The articular

Facets of the pre-sacral vertebrae of *Alligator* had a mean cranial-caudal length of 5.3 mm (s.d. = 0.4), while those of *Varanus* had a mean length of 4.6 mm (s.d. = 0.7); the facet lengths of the two taxa were not significantly different ($t = 1.58$, $n = 5$, $\rho = 0.077$). In *Varanus* the articular facets formed a mean of 25.2% of the vertebral length (s.d. = 3.4) while in *Alligator* the articular facets accounted for only 19.7% of the pre-sacral vertebral length (s.d. = 2.2). The difference in relative facet length was significant ($t = 3.04$, $n = 5$, $\rho = 0.0079$). The pre-sacral vertebrae of *Alligator* are formed from very shallow amphicoelous centra, that are nearly acoelous (Figure 3); in contrast, the centra of *Varanus* are procoelous with a prominent concavity on the anterior surface and convexity on the posterior surface (Figure 3).

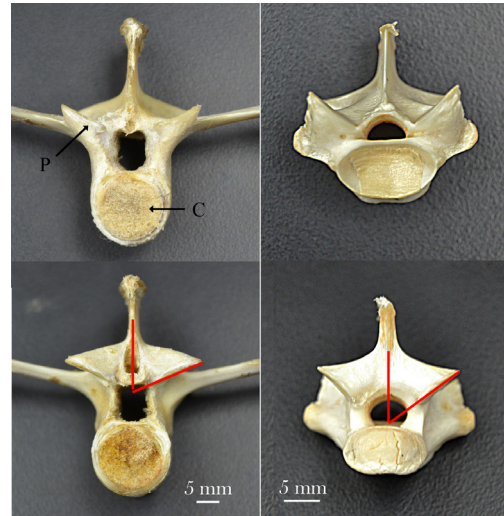


Figure 3. Pre-sacral vertebrae of *Alligator* (left) and *Varanus* (right); the cranial surface is above, the caudal surface below. Red lines indicate the angles of the articular facets. C - centrum; P - articular processes

In *Alligator* the opposing centra of the intervertebral joint are joined by an intervertebral disc of dense irregular connective tissue, fibrocartilage, and a small group of nucleus pulposus cells (Figure 4). The disc is uniform in the middle of the intervertebral joint; on the periphery the dense connective tissue coalesces as a band around the joint. There is no intervertebral disc in *Varanus*; the opposing surfaces of the centra are covered with hyaline cartilage, and a “capsule” of dense connective tissue surrounds the joint.

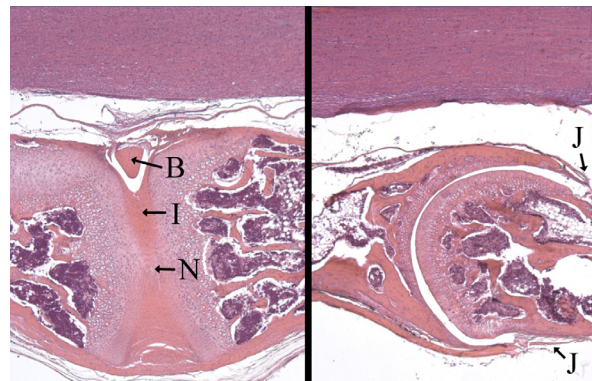


Figure 4. Sagittal sections through the intervertebral joint of *Alligator* (left) and *Varanus* (right); the spinal cord is evident on the top of both images. B - band of dense connective tissue; I - intervertebral disc; J - joint capsule; N - nucleus pulposus

The differences in the intervertebral joints between the centra are apparent when viewing the ventral surface of the vertebral column. In *Alligator* the intervertebral joints are marked by the symmetrical expansions of the connective tissue of the intervertebral disc, while in *Varanus* the ventral surface of the vertebral column is more planar, and the shape

of the centra, and the cavity between them, clearly visible (Figure 5) through the nearly translucent joint capsule.

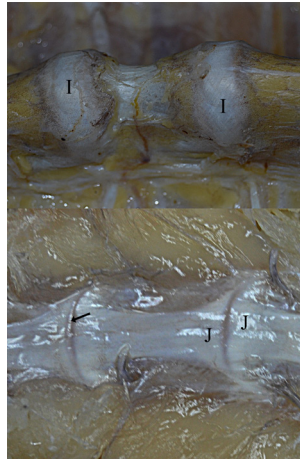


Figure 5. Ventral view of the intervertebral joints of *Alligator* (above) and *Varanus* (below). I - intervertebral disc; J - joint capsule. Note that the joint capsule in *Varanus* is so thin that the articular cartilage and joint cavity are visible through the capsule (arrow)

The (presumed) arachnoid of *Alligator* was highly pigmented (Figure 6). There is a large amount of adipose tissue associated with the dura mater and the IVF. Removal of the adipose reveals connective tissue elements crossing the medial border of the IVF, partitioning the IVF into a large number of small passageways. If this connective tissue is removed, and the spinal nerve exposed within the IVF, the roughly ovoid shape of the IVF of *Alligator* becomes clear (Figure 6).

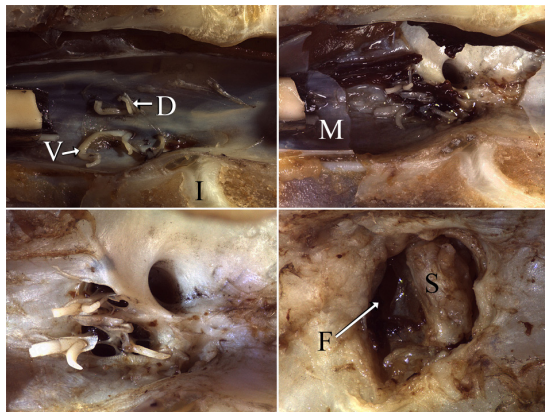


Figure 6. The morphology of the intervertebral foramen of *Alligator*. The sequential images represent a series of medial-lateral dissections beginning at a parasagittal plane through the spinal cord and ending near the mid-point of the intervertebral foramen. D - dorsal nerve root; F - intervertebral foramen; M - meninges (dura mater); S - spinal nerve; V - ventral nerve root

There was no meningeal pigmentation evident in *Varanus* (Figure 7). As the dura extends laterally along the spinal nerve, there is a thickened band of connective tissue

that anchors the anterior surface of the dura to the adjacent vertebra. There are no prominent connective tissue septa or partitions over the medial surface of the IVF in *Varanus*, and there is relatively less adipose in the IVF of this genus. The IVF of *Varanus* is nearly lunate, with the spinal nerve being centrally located (Figure 7).

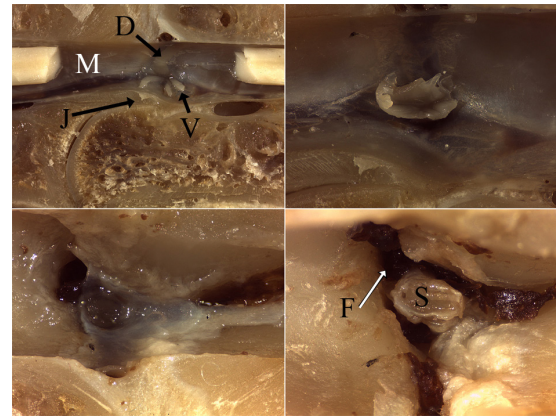


Figure 7. The morphology of the intervertebral foramen of *Varanus*. The sequential images represent a series of medial-lateral dissections beginning at a parasagittal plane through the spinal cord and ending near the mid-point of the intervertebral foramen. D - dorsal nerve root; F - intervertebral foramen; M - meninges (dura mater); S - spinal nerve; V - ventral nerve root

3.2 Biomechanics

Each compression test was repeated for three trials. The three trials yielded relatively consistent results, particularly among the specimens of *Alligator*. In the three trials shown in Figure 8, the maximum stress values ranged from 1296-1493 kPa, the maximum facet displacements ranged from 35.3-41.4%, and the stress per unit displacement values ranged from 31.3-42.5. There was no order effect evident in the three trials.

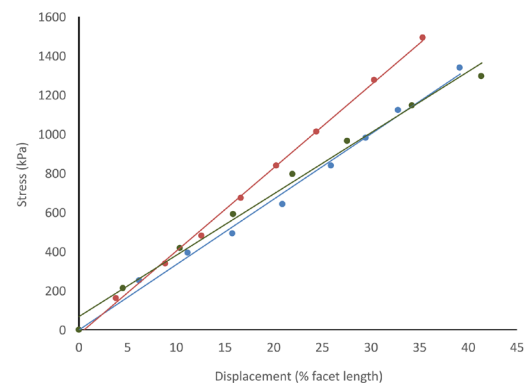


Figure 8. Three compressive trials performed on the same vertebral block from a specimen of *Varanus niloticus*. No “order effect” was observed during any of the compression trials

The compression trials produced a tightly clustered data set from *A. mississippiensis*, and more diversity among the *Varanus* data (Figure 9). In the pooled data set *Varanus* had a mean displacement of 25% of facet length (s.d. = 10.3), while *Alligator* had a mean displacement of 16.6 % of facet length (s.d. = 4.9). The differences in facet displacement between the two groups was significant ($t = 2.83, n = 15, \rho = 0.0043$). In the pooled data set *Alligator* had a mean maximal stress value of 163.4 kPa (s.d. = 65), while *Varanus* had a mean maximal stress value of 1000 kPa (s.d. = 311). The differences in maximal stress between the two groups was significant ($t = 10.2, n = 15, \rho < 0.00001$). The pooled data from *Varanus* had a mean stress per unit displacement of 43.5 (kPa per % facet length displacement) with a s.d. of 15.3; the pooled data from *Alligator* had a mean of 9.9 (s.d. = 3.0). The differences in the stress per unit of facet displacement between the two taxa was significant ($t = 8.32, n = 15, \rho < 0.00001$).

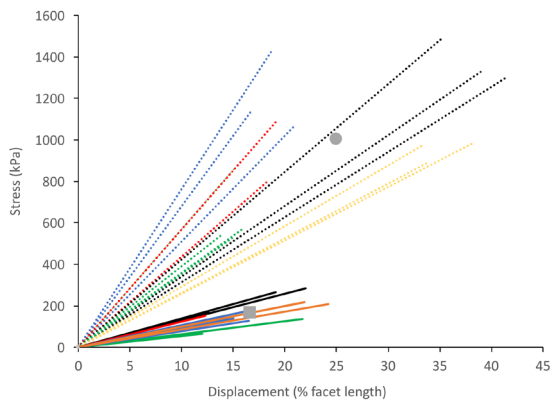


Figure 9. Summary figure of the compression trials. The three separate trials for each specimen are indicated by color coding; data from *Varanus* is indicated by dashed lines, data from *Alligator* in solid lines. Note that some of the data traces are obscured by overlapping lines. The pooled mean for the *Varanus* trials is indicated by the grey circle, the pooled mean for the *Alligator* trials is indicated by the grey square

As evident in Figure 9, the data from *Varanus* was more variable than that from *Alligator*. As noted above, the *Varanus* specimens were drawn from three species, and covered a greater size range than the specimens of *Alligator*. Regression analysis was performed to examine possible influences of body size on the facet biomechanics. As expected, facet size increased with body size; however, compression stress and stress per unit displacement both decreased with body size (Figure 10). The decrease in stress per unit displacement (-5 kPa per % facet length per kg body mass) was significantly different from zero ($F = 24.5, n = 5, \rho = 0.016$). The specimens ranged in mass by 6 kg, suggesting the larger specimen should have a stress per unit displacement

values that is roughly 30 kPa per % facet length lower than the smaller; the actual values range from 64.6 - 27.1 kPa per % facet length. A similar regression analysis was performed on the *Alligator* data set, but no significant relationships with body mass were found.

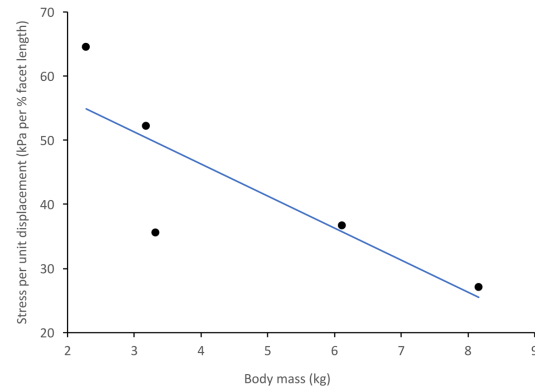


Figure 10. Mean values for the stress per unit displacement (Y axis) plotted against body mass (X axis) for the five specimens of *Varanus*. The slope of the line (-5 kPa per % facet length per kg body mass) is significantly different from 0

Immediately after completing the initial series of compressive trials, the articular facets of the intervertebral joint were physically disrupted and a second set of compressive trials performed. Disrupting the facet joints in *Alligator* caused no significant difference in facet displacement, stress, or stress per unit displacement (Table 1). Disrupting the facet joints in *Varanus* did not significantly alter facet displacement (Table 1); however, both the stress ($t = 2.21, n = 15, \rho = 0.017$) and stress per displacement ($t = 3.58, n = 15, \rho = 0.0006$) were significantly reduced (Table 1).

Table 1. Comparison of facet displacement (% facet length), stress (kPa), and stress per unit displacement (kPa per % facet length) for both *Varanus* and *Alligator* before (intact) and after (crushed) the articular facets were mechanically disrupted. Significant differences are indicated in red; note that only the stress and stress per unit displacement from *Varanus* were significantly different, and that both values decreased after disruption of the facet joints

<i>Varanus</i>			
	disp.	stress	stress/unit disp.
Intact	25 (10.3)	1000.4 (311)	43.5 (15.3)
Crushed	30.6 (7.2)	771.4 (219.7)	26.3 (8.6)
<i>Alligator</i>			
	disp.	stress	stress/unit disp.
Intact	16.7 (4.9)	163.4 (65)	9.9 (3.0)
Crushed	18.4 (6.6)	149.1 (67.9)	7.9 (3.0)

To explore this further, a second round of compression trials were performed using replica vertebrae of *Varanus*. During these trials only the stress per unit displacement

was calculated, and these are presented in relation to an “intact” (baseline) replica system (Table 2). Placing silicone pads within the intervertebral joint between the centra had little to no impact on the stress per unit displacement; in contrast, placing a small sealed pouch of saline in the same location raised the stress per unit displacement sevenfold (Table 2). When displacement of the intervertebral joint at the facets was restricted, so the joint was “fixed”, the stress per unit displacement increased, though only slightly. Cutting the facet joint off of the replica vertebrae reduced the stress per unit displacement, most dramatically in trials with the saline pouch between the centra (Table 2).

Table 2. Stress per unit displacement values determined for compression trials using replica *Varanus* vertebrae. Placing a saline pouch within the intervertebral joint raised the stress per unit displacement values (red)

	plain	thin pad	thick pad	saline
baseline	1.00	0.97	0.94	7.76
fixed	1.30	1.05	1.09	9.82
cut	0.90	0.84	0.78	1.32

3.3 Imaging

The 3D reconstructions made from the CT images provide clear outlines of the intervertebral foramina, as well as sharp anatomical boundaries for quantification with ImageJ (Figure 11). Two vertebral blocks (the CT blocks and the histology blocks) from each specimen were imaged using CT, the histology block was imaged “intact” (with no compression), while the CT block was compressed (by hand) using a C-clamp immediately after excision. This technique produced variation in the amount of compression applied, and the ensuing length change (X-axis of Figure 12). In *Varanus* the CT blocks had a mean length change of 9.4%, while in *Alligator* the mean length change was 12%. The difference in % length change with compression was not significantly different ($T = 1.33$, $p = 0.109$). The surface area of the intervertebral foramen of *Varanus* decreased by 25.3% following compression (Y-axis, Figure 12); in *Alligator* compression reduced the surface area of the intervertebral foramen by 19.3%. The difference in IVF surface area reduction following compression was not significant ($t = 1.73$, $p = 0.06$). Though the mean values were not significantly different, reduction in length was associated with a greater reduction in IVF area in *Varanus*; the slope of this relationship was 2.28 in *Varanus* but 0.33 in *Alligator* (Figure 12). Comparing these two slopes revealed that they were significantly different ($t = 9.56$, $df = 6$, $p = 0.74 \times 10^{-5}$).

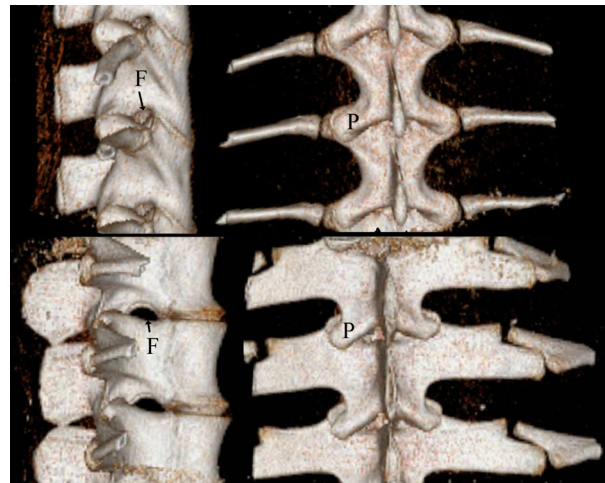


Figure 11. 3D reconstruction of CT images of the same vertebral level from *Varanus* (top) and *Alligator* (bottom); lateral view (left), dorsal view (right). F - intervertebral foramen; P - articular process

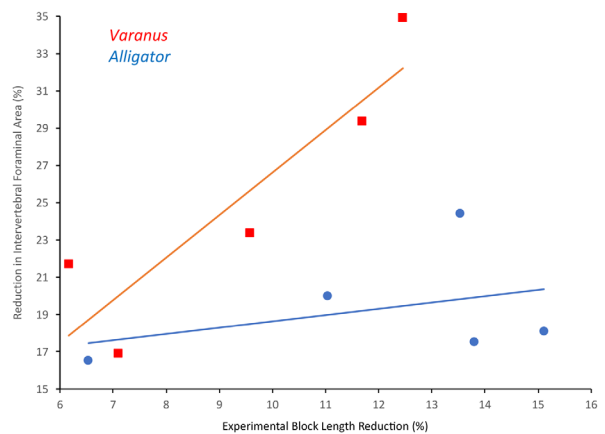


Figure 12. Effect of compression on intervertebral foraminal area from vertebral blocks removed from the same level of the vertebral column of *Varanus* (red) and *Alligator* (blue). The vertebral blocks were imaged with a CT, 3D reconstructions performed, then the reconstructed images quantified using ImageJ

Within the slice parameters afforded by the MRI the “same” images from all three of the compressive trials for each MRI block were quantified (Figure 13). During the MRI compression trials the mean length of the *Alligator* vertebral units changed from 20.9 to 19.7mm, a change of 5.9%. This change in length was associated with a decrease in IVF surface area from 21.8 to 19.1mm², a decrease of 12%. The compression trials caused the mean length of the *Varanus* vertebral units to change from 13.9 to 13.1mm, a change of 5.6%. This change in length was associated with a decrease in IVF surface area from 10.6 to 7.9mm², a decrease of 25.5%. The *Alligator* data had a slope of -2.28, while the *Varanus* data had a slope of

-1.11 (Figure 14). The difference between the two slopes was significant ($t=10.26$, $df = 26$, $p = 1.23 \times 10^{-10}$).

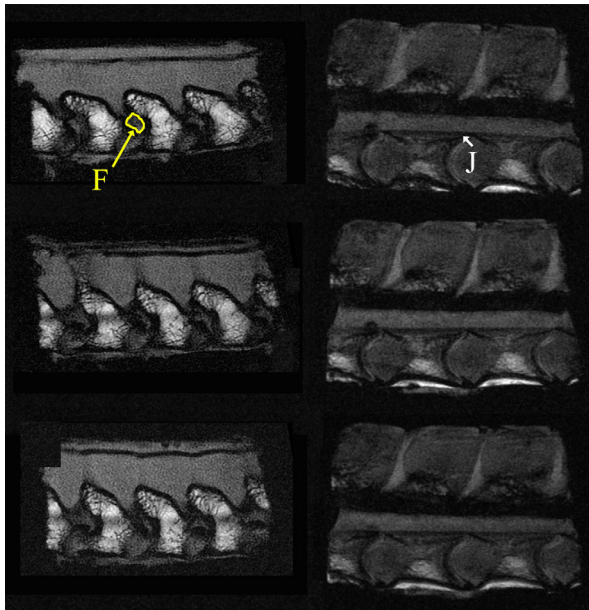


Figure 13. MRI series showing the intervertebral foramina (left) and midline slice (right) that were used to quantify vertebral unit length. Images on the left are from *Alligator*, images on the right are from *Varanus*. In both series compression increased from top to bottom. F - intervertebral foramen; J - joint capsule

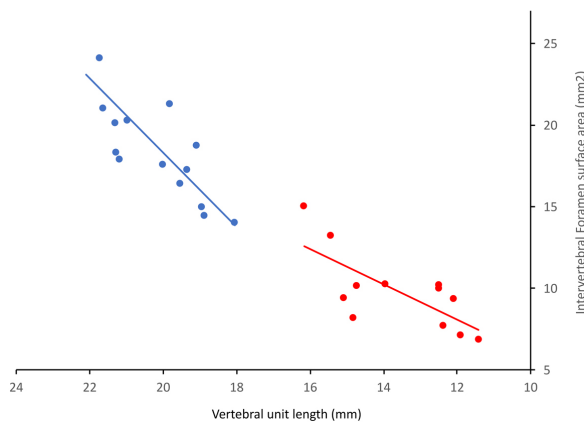


Figure 14. Results of the MRI compression trials showing the vertebral unit length against intervertebral foramen surface area for *Alligator* (blue) and *Varanus* (red) vertebral blocks removed from the same level of the vertebral column. The compression trials were performed by hand, and this data set is not corrected to a mean size, so the three “stages” of the compression are not distinct in the data points

Histological analysis was performed on CT and histology blocks from *Alligator* and *Varanus salvator*. In each pair of blocks (Figure 15), the histology block was left “intact” (non-compressed) while the CT block was com-

pressed (with a C-clamp). In both species the spinal nerve occupies a small fraction of the intervertebral foraminal area (*Varanus* = 5.4%, *Alligator* = 6.8%). The compression performed with the C-clamp produced similar changes in both species with foraminal area decreasing by 57% in *Varanus* and by 62% in *Alligator*. The compression applied to the *Alligator* vertebral blocks produced deformation (bulging) of the intervertebral disc; and in both genera displacement of the articular facets was evident following compression (Figure 15).

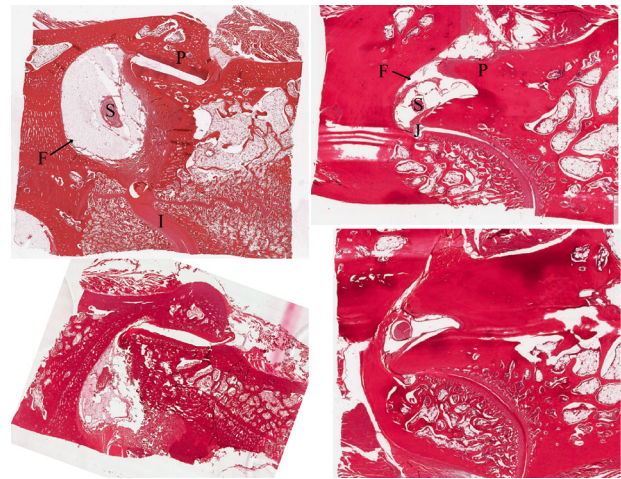


Figure 15. Histological sections through the intervertebral foramen of *Alligator* (left) and *Varanus* (right). Upper images are from the intact (non-compressed) blocks; lower images are from the compressed blocks. F - intervertebral foramen; P - articular process; S - spinal nerve

4. Discussion

The present study focused on the displacement of the articular facets of the intervertebral joint, rather than the biomechanics of the entire vertebral column. This restriction was based on our early observation of the clear physical displacement at this site (Figure 1), the difficulty of quantifying displacement at the more internal and complexly-shaped intervertebral joint between the centra, and the recognition that our testing protocol was not sufficient to quantify the biomechanical properties of the vertebral body. The mobility of the superior articular facet relative to the inferior articular facet in these reptiles meant that in some trials the superior articular facet was initially cranial (so compression reduced the facet joint length) while in other trials the superior articular facet was initially directly over the inferior (so compression actually elongated the facet joint length). For clarity, we quantified the linear displacement of the superior articular facet, and expressed it as % of the facet length (a value that was not influenced by the initial relative positions of the opposing facets).

For the sake of comparison, we can ignore the distinction between facet joint shortening and elongation, and treat the stress per unit displacement determined in this study as Young's Modulus. The values determined for the Young's Modulus of the intervertebral joint (mean 44 kPa for *Varanus*, and 10 kPa for *Alligator*) were well below reported values for compact (~20 GPa) or cancellous (~12 GPa) bone^[34]. This is not surprising given that our methodology was explicitly restricted to the intervertebral joint itself, not the surrounding bone. The experimental values determined for the reptilian intervertebral joint are similar to what has been measured from nucleus pulposus (64.9 kPa) and annulus fibrosus (25.0 kPa) of the human intervertebral disc^[35]. Previous studies of the synovial joint in the inner ear have yielded Young's Moduli ranging from 0.33 - 8.92 MPa^[36], a similar range has been determined from interphalangeal joints^[37,38]. The general similarity of these results to those reported herein for the intervertebral joints of *Varanus* are taken as support for the general methodology employed in this study.

The biomechanical analysis of the intervertebral joints found that the stress per unit displacement of *Varanus* was more than 4x greater than that of *Alligator*, a difference that was significant. Related to this, the maximum stress of *Varanus* was roughly 6x greater than that of *Alligator*, a difference that was also significant. These significant differences were present in the pooled data; these differences would be more pronounced if we corrected the *Varanus* data for body size (Figure 10). Though not commonly treated allometrically, previous studies have described scaling effects in Young's modulus^[39]. The structure of the intervertebral joints in these two groups are very different; *Varanus* has an asymmetric, curved, diarthrotic joint (Figure 1,2) while *Alligator* has a symmetric, nearly flat, synchondrotic joint (Figure 1,2). The diarthrotic intervertebral joints of squamates have frequently been interpreted as facilitating a greater range of vertebral mobility^[11,12], while the *Alligator* intervertebral joint has been interpreted as leading to a stiffening of the body^[7]. This analysis of compression produced the opposite conclusion, with the intervertebral joint of *Varanus* being significantly stiffer than that of *Alligator*. The crocodylian vertebral column has been previously studied to gain insight into the diversity of archosaur locomotion, but these previous studies have concentrated on the shape of the vertebrae, not the intervertebral disc^[40, 41, 42].

Compressive loads acting on the intervertebral joints of *Varanus* and *Alligator* appear to be resisted by very different mechanics. In *Alligator*, the force is resisted by a relatively large symmetrical pad of fibrocartilage and the nucleus pulposus cells. In *Varanus* compression re-

sulted in greater displacement than was recorded in *Alligator*; this displacement both eliminated the gap in the intervertebral joint between the centra, but also displaced the superior articular facet relative to the inferior articular facet (Figure 15). Further compression was resisted both by the hyaline cartilage on the centra, but also by tensile forces acting on the collagenous fibers around the facet joint.

Three lines of evidence support this interpretation of the varanid intervertebral joint. First, the anatomical comparisons between the "normal" and "compressed" intervertebral joint of *Varanus* all revealed marked displacement at the facet joint, and a structural change in the joint capsule on the cranial surface of the facet joint where tension would be acting (Figure 15). Second, experimental disruption of the facet joint, so that compression would have been resisted primarily/solely by the opposing central surfaces, resulted in a significant decrease in the stress per unit displacement (Table 1). Third, in the studies performed with the replica vertebrae the condition of the facet joint (fixed versus absent) produced a corresponding change in the stress per unit displacement (Table 2).

A major questions of this project was, "How do large squamate reptiles, like *Varanus*, withstand spinal compression when moving in an upright (bipedal) posture?" The reduction in foraminal area that occurs during compression in *Varanus* (25.3 %) is greater than what is seen during foraminal stenosis in humans and other mammals^[24]. Since the intervertebral foramen is defined, in part, by the articular facet joint, the large displacement at this joint in *Varanus* should result in a significance change in foraminal area. The results of this study suggest that the neuromuscular integrity of a bipedal varanid is maintained by a combination of three factors: First, the facet joint limits physical displacement at the intervertebral joint. Second, the spinal neurovascular bundle occupies a relatively small percentage of the foraminal area (5.4%); in humans the neurovascular bundle can occupy over 50% of the foraminal area^[43,44] and the ratio of neural size to foraminal area is considered a good predictor of impingement^[24]. The fat and space surrounding the spinal neurovascular bundle of *Varanus* provides a compressive boundary to the nerves. Third, the spinal nerve of *Varanus* is not as "bound" by connective tissue as is the human spinal nerve. The circumneural sheath and fibrous operculum of the mammalian intervertebral foramen^[45,46] are not found, or at least are not as well-developed, in *Varanus*. This gives the spinal nerve of *Varanus* greater physical flexibility and increases the opportunity for the nerve to physically move during foraminal restriction to minimize, if not avoid, impingement.

5. Conclusion

Morphological variation among the intervertebral joints of different reptilian taxa can lead to sharp differences in biomechanics, in both range of motion and compression resistance. Variation in the vertebral biomechanics has influenced the ecological and locomotor diversification of reptiles.

Funding

There was no external funding for this research.

Conflict of Interest

The authors declare that they have no conflict of interest associated with this research.

Availability of Data

Data will be provided upon reasonable requests to the corresponding author.

Code Availability

Not applicable.

Author's Contribution

Kadi Fauble: The author contributed to study design, data collection and analysis, imaging, and writing of the manuscript.

James Adams: The author contributed to data analysis, imaging, and writing of the manuscript.

Maura Gerdes: The author contributed to data collection, imaging, and writing of the manuscript.

Caroline VanSickle: The author contributed to study design, data analysis, and writing of the manuscript.

Bruce A. Young: The author contributed to study design, data collection and analysis, imaging, and writing of the manuscript.

Ethics Approval

The husbandry and use of the live animals followed all applicable national guidelines, and was approved by the IACUC of A.T. Still University (Protocols #208 and #209).

Consent to Participate

All authors agree to participate in this study

Consent for Publication

All authors agree to the publication of this study.

Acknowledgments

The authors wish to thank R. Elsey of the Louisiana Department of Wildlife and Fisheries and P. Kondrashov for their support, and J. Carroll for his assistance with the replica vertebrae.

References

- [1] Parrish JM. The Origin of Crocodylian Locomotion. *Paleobiology*, 1987, 13: 396-414.
- [2] Bell G, Polcyn M. *Dallasaurus Turneri*, a New Primitive Mosasauroid from the Middle Turonian of Texas and Comments on the Phylogeny of Mosasauridae (Squamata). *Neth J Geosci*, 2005, 84: 177-194.
- [3] Caldwell MW. From Fins to Limbs to Fins: Limb Evolution in Fossil Marine Reptiles. *Amer J Med Genet*. 2002, 112: 236-249.
- [4] Motani R. The Evolution of Marine Reptiles. *Evol Educ Out*, 2009, 2: 224-235.
- [5] Molnar J, Pierce S, Hutchinson J. An Experimental and Morphometric Test of the Relationship between Vertebral Morphology and Joint Stiffness in Nile Crocodiles (*Crocodylus Niloticus*). *J Exp Biol*, 2014, 217: 758-768.
- [6] Molnar J, Pierce S, Bhullar B-A, Turner A, Hutchinson J. Morphological and Functional Changes in the Vertebral Column with Increasing Aquatic Adaptation in Crocodylomorphs. *Roy Soc Open Sci*, 2015, 2: 150439.
- [7] Frey E. The Carrying System of Crocodylians - a Biomechanical and Phylogenetic Analysis. *Stuttgart Beit Naturkund Biol*, 1988, 426: 1-60.
- [8] Hoffstetter R, Gasc J-P. Vertebrae and Ribs of Modern Reptiles. In - *Biology of the Reptilia*, Vol. 1, pp. 201-310. 1969, Academic Press, New York.
- [9] Haines RW. The Development of Joints. *J Anat*, 1947, 81: 33-55.
- [10] Werner YL. The Ontogenic Development of the Vertebrae in Some Gekkonoid Lizards. *J Morphol*, 1971, 133: 41-91.
- [11] Taylor M, Wadel M. The Effect of Intervertebral Cartilage on Neutral Posture and Range of Motion in the Necks of Sauropod Dinosaurs. *PLoS One*, 2013. DOI: 10.1371/journal.pone.0078214
- [12] Morinaga G, Bergmann PJ. Angles and Waves: Intervertebral Joint Angles and Axial Kinematics of Limbed Lizards, Limbless Lizards, and Snakes. *Zoology*, 2019, 134: 16-26.
- [13] Persons WS, Currie PJ. The Functional Origin of Dinosaur Bipedalism: Cumulative Evidence from Bipedally Inclined Reptiles and Disinclined Mammals. *J Theor Biol*, 2017, 420: 1-7.

- [14] Gauthier JA, Nesbitt SJ, Schachner ER, Bever GS, Joyce WG. The Bipedal Stem Crocodylian *Poposaurus Gracilis*: Inferring Function in Fossils and Innovation in Archosaur Locomotion. *Bull Peabody Mus Nat Hist*, 2011, 52: 107-126.
- [15] Snyder RC. Adaptations For Bipedal Locomotion Of Lizards. *Amer Zool*, 1962, 2: 191-203.
- [16] Schuett GW, Reiserer RS, Earley RL. The Evolution of Bipedal Postures in Varanoid Lizards. *Biol J Linn Soc*, 2009, 97: 652-663.
- [17] Currey J. Comparative Mechanical Properties and Histology of Bone. *Amer Zool*, 1984, 24: 5-12.
- [18] Nicholson P, Cheng X, Lowet G, Boonen S, Davie M, et al., Structural and Material Mechanical Properties of Human Vertebral Cancellous Bone. *Med Engin Physics*, 1997, 19: 729-737.
- [19] Blob RW, Snelgrove JM. Antler Stiffness in Moose (*Alces alces*): Correlated Evolution of Bone Function and Material Properties? *J Morph*, 2006, 267: 1075-1086.
- [20] Leone A, Guglielmi G, Cassar-Pullicino VN, Bonomo L. Lumbar Intervertebral Instability: A Review. *Radiology*, 2007, 245: 62-77.
- [21] Howarth SJ, Callaghan JP. Compressive Force Magnitude and Intervertebral Joint Flexion/Extension Angle Influence Shear Failure Force Magnitude in the Porcine Cervical Spine. *J Biomech*, 2012, 45: 484-490.
- [22] Moon BR. Testing an Inference of Function from Structure: Snake Vertebrae Do the Twist. *J Morph*, 1999, 241: 217-225.
- [23] Crock H. Normal and Pathological Anatomy of the Lumbar Spinal Nerve Root Canals. *J Bone Joint Surg*, 1981, 63B: 487-490.
- [24] Jenis LG, An HS. Lumbar Foraminal Stenosis. *Spine*, 2000, 25: 389-394.
- [25] Jensen K, Mosekilde L, Mosekilde L. A Model of Vertebral Trabecular Bone Architecture and Its Mechanical Properties. *Bone*, 1990, 11: 417-423.
- [26] Goel VK, Ramirez SA, Kong W, Gilbertson LG. Cancellous Bone Young's Modulus Variation Within the Vertebral Body of a Ligamentous Lumbar Spine-Application of Bone Adaptive Remodeling Concepts. *J Biomech Engin*, 1995, 117: 266-271.
- [27] Haj-Ali R, Massarwa E, Aboudi J, Galbusera F, Wolfram U, et al., A New Multiscale Micromechanical Model of Vertebral Trabecular Bones. *Biomech Model Mechanobiol*, 2016, 16: 933-946.
- [28] Hoffman B, Martin M, Brown BN, Bonassar LJ, Cheatham J. Biomechanical and Biochemical Characterization of Porcine Tracheal Cartilage. *Laryngoscope*, 2016, 126: E325-E331.
- [29] Bae WC, Ruangchaijatuporn T, Chang EY, Biswas R, Du J, et al., Morphology of Triangular Fibrocartilage Complex: Correlation with Quantitative MR and Biomechanical Properties. *Skel Radiol*, 2015, 45: 447-454.
- [30] Koike T, Wada H. Modeling of the Human Middle Ear Using Finite-Element Method. *J Acoust Soc Amer*, 2002, 111: DOI: 10.1121/1.1451073
- [31] Barfuss D, Dantzer W. Glucose Transport in Isolated Perfused Proximal Tubules of Snake Kidney. *Amer J Physiol*, 1976, 231: 1716-1728.
- [32] Han D, Young BA. The rhinoceros among serpents: Comparative anatomy and experimental biophysics of Calabar burrowing python (*Calabaria reinhardtii*) skin. *J Morph*, 2017, 279: 86-96.
- [33] Luna, LG. Manual of Histological Staining Methods of the Armed Forces Institute of Pathology. 1968, McGraw-Hill, New York.
- [34] Rho JY, Ashman RB, Turner CH. Young's Modulus of Trabecular and Cortical Bone Material: Ultrasonic and Microtensile Measurements. *J Biomech*, 1998, 26: 111-119.
- [35] Cortes DH, Jacobs NT, Delucca JF, Elliott DM. Elastic, Permeability and Swelling Properties of Human Intervertebral Disc Tissues: A Benchmark for Tissue Engineering. *J Biomech*, 2014, 47: 2088-2094.
- [36] Zhang X, Gan RZ. Experimental Measurement and Modeling Analysis on Mechanical Properties of Incudostapedial Joint. *Biomech Model Mechanobiol*, 2010, 10: 713-726.
- [37] Hashizume H, Akagi T, Watanabe H, Inoue H, Ogura T. Stress Analysis of PIP Joints Using the Three-Dimensional Finite Element Method. In - *Advances in the Biomechanics of the Hand and Wrist*. pp 237-244. 1994, Springer, New York.
- [38] Fowler N, Nicol A. Interphalangeal Joint and Tendon Forces: Normal Model and Biomechanical Consequences of Surgical Reconstruction. *J Biomech*, 2000, 33: 1055-1062.
- [39] Doube M, Klosowski MM, Wiktorowicz-Conroy AM, Hutchinson JR, Shefelbine SJ. Trabecular bone scales allometrically in mammals and birds. *Proc Royal Soc B*, 2011, 278: 3067-3073.
- [40] Salisbury S, Frey E. A biomechanical transformation model for the evolution of semi-spheroidal articulations between adjoining vertebral bodies in crocodylians. In - *Crocodylian Biology and Evolution*. pp. 85-134. 2000, Surrey Beatty & Sons: Chipping Norton, UK.
- [41] Iijima M, Kubo T. Comparative morphology of presacral vertebrae in extant crocodylians: taxonomic, functional and ecological implications. *Zool J Linn*

- an Soc, 2019, 186: 1006-1025.
- [42] Fronimos JA, Wilson JA. Concavo-convex intercentral joints stabilize the vertebral column in sauropod dinosaurs and crocodylians. *Ameghiniana*, 2017, 54: 151-176.
- [43] Sunderland S. Meningeal-Neural Relations in the Intervertebral Foramen. *J Neurosurg*, 1974, 40: 756-763.
- [44] Stephens M, Evans JH, O'brien JP. Lumbar Intervertebral Foramens. *Spine*, 1991, 16: 525-529.
- [45] Wiltse LL, Fonseca AS, Amster J, Dimartino P, Ravessoud FA. Relationship of the Dura, Hofmann's Ligaments, Batson's Plexus, and a Fibrovascular Membrane Lying on the Posterior Surface of the Vertebral Bodies and Attaching to the Deep Layer of the Posterior Longitudinal Ligament. *Spine*, 1998, 18: 1030-1043.
- [46] Jagla G, Walocha J, Rajda K, Dobrogowski J, Wordliczek J. Anatomical Aspects of Epidural and Spinal Analgesia. *Adv Pall Med*, 2009, 8: 135-146.